J Mater Sci (2007) 42:9638–9644
DOI 10.1007/s10853-007-1970-6

Growth of highly oriented ZnO films by the two-step electrodeposition technique

Xiang-Dong Gao · Fang Peng · Xiao-Min Li · Wei-Dong Yu · Ji-Jun Qiu

Received: 18 May 2007 / Accepted: 26 June 2007 / Published online: 31 July 2007
© Springer Science+Business Media, LLC 2007

Abstract Compact and transparent ZnO films were deposited on the ITO/glass substrates from zinc nitrate aqueous solution by the two-step electrodeposition technique. While the first potentiostatic step was used to produce ZnO seed layer, the ZnO film growth has been done galvanostatically. Effects of the potentiostatic parameters on the crystal structure, morphology and optical properties of ZnO films were investigated. Results show that ZnO films with highly *c*-axis preferred orientation can been obtained when the potentiostatic deposition at –1.2 V for 15 s has been applied. Such an observation might be attributed to the etching process of ITO substrate in the diluted HCl solution. The film exhibits smooth and compact morphology, high transmittance in the visible band (>80%) and sharp absorption edge (at ~370 nm). The analysis on the growth mechanism indicates that the short potentiostatic process prior to the film growth can produce ZnO seed layer and substitute the initial nucleation process in the conventional one-step galvanostatic deposition, thus increasing the nucleation density and preventing the formation of loose structures.

X.-D. Gao · F. Peng · X.-M. Li (✉) · W.-D. Yu · J.-J. Qiu
State Key Laboratory of High Performance Ceramics and Superfine Microstructures, Shanghai Institute of Ceramics, Chinese Academy of Sciences, Shanghai 200050, China
e-mail: lixm@mail.sic.ac.cn

F. Peng
Graduate school of Chinese Academy of Sciences, Beijing 100039, China

Introduction

Zinc oxide (ZnO) films have attracted much attention for numerous applications such as piezoelectric transducers, short wavelength optical devices, chemical sensors and photovoltaic cell [1–3]. Especially, in photovoltaic cells, ZnO films are used as transparent conducting electrodes in thin film solar cells based on copper indium diselenide [4] or amorphous silicon [5].

Many techniques have been applied to fabricate ZnO films, such as sputtering [6], molecular beam epitaxy [7], pulsed laser deposition [8], metal organic chemical vapor deposition [9], filtered vacuum arc deposition [10], and spray pyrolysis [11]. Recently, the cathodic electrodeposition of ZnO films has induced considerable interests due to its distinctive advantages such as: the precise control over the film thickness and morphology, the possibility to prepare films with large area, relatively high deposition rate, low growth temperature, and low cost [12–23].

The most important aspect in the electrochemical deposition of ZnO films is the reduction of an oxygen precursor at the interface of electrode and precursor solution, which controls the growth rate, and affects the crystallinity and morphology of the obtained film significantly. Three kinds of oxygen precursor have been reported up to now, i.e., nitrate ions [3, 13–16], dissolved molecular oxygen [1, 12, 17–21], and hydrogen peroxide [18, 22]. Among them, nitrate ions-based oxygen precursor has received considerable interests [3, 13–16, 23]. Compared with the dissolved molecular oxygen precursor, the zinc nitrate solution can act as both the zinc and oxygen precursor, which will simplify the electrolyte composition, and widen the adjustable range of oxygen concentration. However, for the nitrate ions-based oxygen precursor, compact and transparent ZnO films could not be easily

obtained by the mere galvanostatic or potentiostatic deposition method [3, 13, 14, 23]. In 1999, Izaki et al. have proposed an effective two-step electrolysis to prepare dense and defect-free ZnO films, which consists of the pretreatment on the substrate at more negative potential for nucleation, and subsequent film growth by potentiostatic deposition at the less negative potential [24]. However, few reports have been found in literature focusing on the galvanostatic deposition mode and the nucleation of ZnO induced by the electrochemical pretreatment. Compared with the potentiostatic deposition, the galvanostatic deposition technique is favorable for its precise control over the deposition current and the growth rate of the films. So a detail investigation on this field is both interesting and technologically important.

In the present work, we have demonstrated the technique to grow ZnO films from zinc nitrate aqueous solution, by applying the potentiostatic process for the nucleation process and the galvanostatic deposition for film growth. Effects of the potentiostatic parameter on the structure, morphology and optical properties of ZnO films were investigated in detail. The nucleation process and formation mechanism of ZnO film were discussed by analyzing the current-time curve during the electrochemical process and the surface morphology of the film at the early stage.

Experimental details

ZnO films were electrodeposited on indium-tin oxide (ITO)/glass substrates in the aqueous solution of zinc nitrate hexahydrate (0.1 M $Zn(NO_3)_2 \cdot 6H_2O$, A.R.) with the pH adjusted to about 6.0 by NaOH solution. The electrochemical deposition was performed in a conventional electrochemical reaction cell with a standard three-electrode configuration. ITO/glass substrates (about 1.5 cm × 1.5 cm), a platinum sheet (99.99%) and a saturated calomel electrode (SCE) in saturated KCl solution were employed as the work, counter and reference electrode, respectively. The deposition temperature was maintained at 80 ± 2 °C by a thermostat. Prior to the deposition, the ITO/glass substrates were ultrasonically rinsed in acetone, alcohol and distilled water first, and then etched in the diluted hydrochloric acid (5–6%) for 10 s, and finally rinsed in distilled water. To make a comparison, the control sample deposited on substrate without the etching in diluted HCl was prepared.

The deposition of ZnO films consisted of two steps, i.e., the potentiostatic process for a short time (referred as the pretreatment in the following text), and the galvanostatic deposition for the film growth. For the pretreatment process, the applied potential is more cathodic than that commonly-required for the deposition of ZnO, and typically two cathodic potentials (–1.2 V, –1.4 V) and three times (5 s, 15 s, 60 s) were chosen. For the subsequent galvanostatic deposition process, the current density was maintained at –0.5 $mA.cm^{-2}$ and deposition time at 20 min.

The electrochemical deposition process was performed by the Electrochemical Autolab (CHI660B, CH Instrument, Inc.), which could also record the current-time or potential-time curves. The crystalline structure characterization of ZnO thin films was carried out by X-ray diffraction (Model D/max 2200 PC with Cu Ka, Rigaku Co., Tokyo, Japan). The morphologies of surface and cross section were analyzed by field emission scanning electron microscope (SEM) (JSM-6700F). Optical properties were characterized by transmittance spectra measured using spectrophotometer (Shimadzu Ltd., UV-3101PC, Japan) in the wavelength range of 200–800 nm. An ITO/glass substrate was placed in the reference optical path to compensate the light intensity.

Results and discussions

Crystalline structure

Figure 1 shows the influence of the potentiostatic pretreatment conditions on the crystalline structure of ZnO films as characterized by XRD pattern. Apart from the characteristic peaks of ITO substrate, only one peak of wurtzite ZnO could be observed distinctly. ZnO films both with and without the pretreatment showed (002) preferred orientation. The intensity of (002) diffraction peak in ZnO film can be used to evaluate the effects of pretreatment process in view of the relatively short pretreatment time

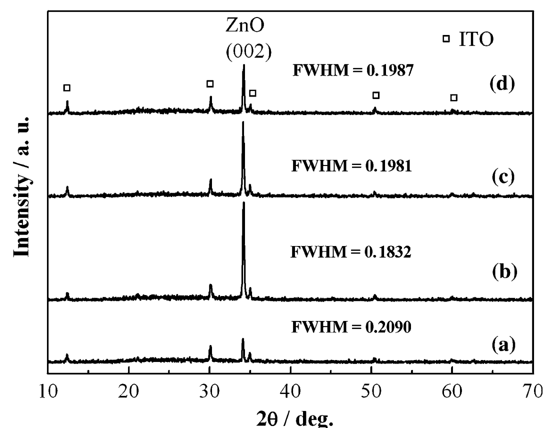

Fig. 1 XRD patterns of electrodeposited ZnO films prepared (**a**) without pretreatment, and with different pretreatment conditions: (**b**) –1.2 V for 15 s, (**c**) –1.4 V for 15 s, and (**d**) –1.2 V for 5 s

(usually less than one minute) and the subsequent identical deposition condition. Compared with the film without pretreatment, the intensity of (002) diffraction peak of ZnO film with pretreatment was significantly enhanced. Also the intensity of (002) peak varied with the pretreatment potential and time, that is, the intensity decreased when the potential became more cathodic or the pretreatment time increased, indicating the change of the crystalline degree of the film. At the pretreatment condition of –1.2 V for 15 s, ZnO film exhibited the highest crystallinity.

The crystallite size of ZnO can be estimated on the basis of Scherrer's relation [25] and full-width half-maximum (FWHM) data shown in Fig. 1. The size of primary ZnO crystallites for the film without the pretreatment, and with the pretreatment of –1.2 V 15 s, –1.4 V 15 s, and –1.2 V 5 s was 41.5, 47.4, 43.8, and 43.6 nm, respectively. An obvious increase in the primary crystallite size can be observed. We think the increase of primary crystallites after the pretreatment may be related to the more cathodic potential applied during the nucleation stage than the case without the pretreatment.

It should be also noticed that, all the ZnO films grown in this work exhibited the strong preferential orientation along *c*-axis, which is not very common for electrodeposited ZnO films from zinc nitrate solution [3, 13, 23]. Because no direct relationship between the preferential orientation and the pretreatment could be found, we started to examine other experimental parameters influencing the crystallization of ZnO film. It was found that the etching of ITO substrate in diluted hydrochloric acid (HCl) is the immediate cause of the orientation. For ZnO film deposited on ITO substrate without the etching process in diluted HCl (with the potentiostatic pretreatment of –1.2 V 15 s), three diffraction peaks along (100), (101) and (102) plane can be clearly observed except (002) peak, as shown in Fig. 2. The

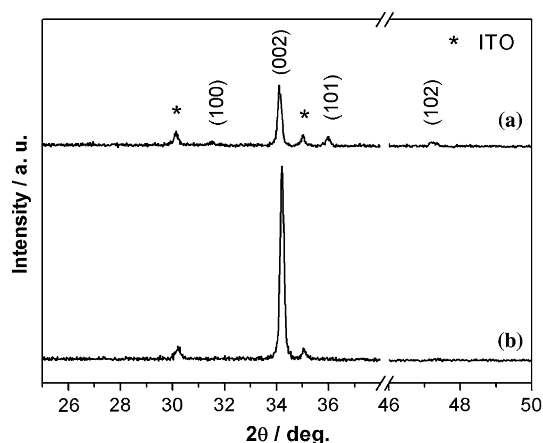

Fig. 2 XRD patterns of electrodeposited ZnO films prepared on ITO substrate (**a**) without and (**b**) with etching process in diluted HCl (5–6%) for 10 s. Pretreatment condition: –1.2 V for 15 s

underlying mechanism can be explained as follows. In the $ZnNO_3$ based electrochemical system, ZnO can be formed at cathode through following reactions:

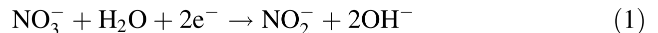

$$NO_3^- + H_2O + 2e^- \rightarrow NO_2^- + 2OH^- \quad (1)$$

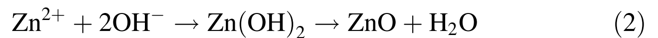

$$Zn^{2+} + 2OH^- \rightarrow Zn(OH)_2 \rightarrow ZnO + H_2O \quad (2)$$

It is known that the growth of ZnO along (002) plane possesses the lowest energy compared with the growth along other planes. Many researches have observed that the orientation of ZnO film along (002) plane can be obtained by increasing the temperature in spray pyrolysis [26] or electrochemical deposition methods [21], which would be expected to improve the driving force of ZnO to accommodate the lattice sites with the lowest energy. However, the orientation of ZnO film in this work cannot be explained by the temperature rise. We think the increase of the surface energy on ITO substrate due to its etching in diluted HCl may be responsible for the underlying reasons. It has been confirmed that the ITO layer on glass (~200 nm) can be fully removed by immersion in diluted HCl for 1 min. So the etching of ITO substrate in diluted HCl for 10 s will peel off the "old" surface by dissolve the ITO layer, exposing the "fresh" surface. The fresh surface possesses a large quantity of dangling bond (In^{3+}), which has the great tendency to react with oxygen, to lower the surface energy. In the electrodeposition process of ZnO film, this is equivalent to the decrease of the activation energy for the formation of ZnO, which will promote the preferential orientation of ZnO along the lowest energy. In addition, the newly-exposed ITO surface may be also much coarser than the original one because of the very rapid corrosion rate. The coarse surface possesses higher energy than the smooth one, which is also beneficial for the orientation of ZnO film.

Morphology

Figure 3a–d shows SEM images of electrodeposited ZnO films on surface and cross section with and without electrochemical pretreatment. For the film without pretreatment, the obtained layer exhibited an open structure composed of separate columnar rods with a well-defined hexagonal cross section. The distribution density of rods on the substrate was low and the average size of ZnO rod was 500 nm. For the film with pretreatment, the dense film structure was obtained, with the crystallite size decreasing remarkably. That is to say, the pretreatment process favors the formation of dense ZnO films. With the pretreatment of –1.2 V for 15 s, the hexagonal shape of crystallites disappeared, all ZnO crystallites were packed compactly, and

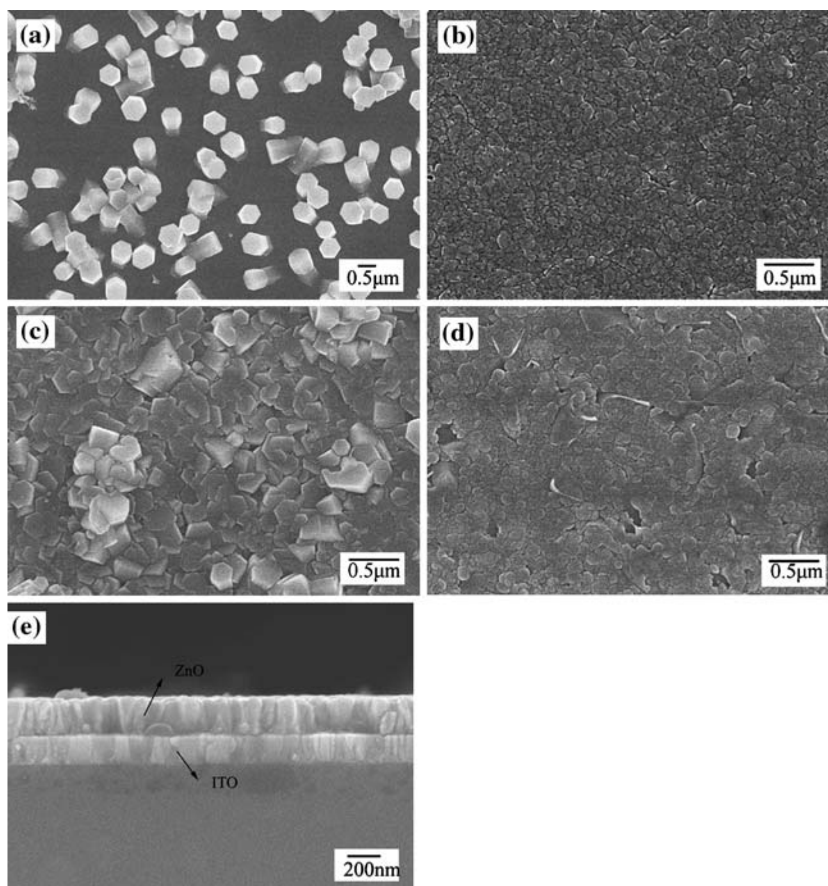

Fig. 3 SEM images of electrodeposited ZnO films as a function of the pretreatment conditions: (**a**) without pretreatment, (**b**) –1.2 V, 15 s, (**c**) –1.4 V, 15 s, (**d**) –1.2 V, 5 s, and (**e**) cross-section structure of ZnO film obtained under the condition of (**b**)

no pores or defects could be observed. The average value of particle size was less than 100 nm. With the pretreatment of –1.4 V for 15 s, the film structure was dense as well. However, ZnO particles exhibited the hexagonal shape, with the size increasing to about 250 nm. With the pretreatment of 1.2 V for shorter (5 s) or longer (60 s, not shown) time, the particle size increased and the degree of compactness of the film decreased slightly.

Above morphological analysis indicated that, after the electrochemical pretreatment, the size of secondary ZnO particles decreased, and the quantity increased. This was related to the formation of ZnO crystallites during the pretreatment course (as shown in Section ''Analysis on growth mechanism''), which will increase the nuclei density of ZnO on ITO during the film growth course and prevent the growth of large secondary particles. It can be also found that the film with different pretreatment exhibited different morphology, and the application of higher voltage (–1.4 V) or shorter time (5 s) resulted in the larger secondary particles. The higher voltage will produce higher current density, resulting in the formation of more ZnO crystallites in the same time slit. Then the primary ZnO crystallites will tend to amalgamate together and form larger particles. For the shorter pretreatment time, it may be not enough to produce large quantity of crystallites on substrate. Then the coalescence of neighboring crystallites will be significant, resulting in the formation of large particles.

Figure 3e gives the cross section structure of ZnO film obtained with the pretreatment under the condition of –1.2 V for 15 s. The film was composed of dense column particles perpendicular to the substrate, which agrees well with result of XRD patterns. The film thickness was about 250 nm and the growth rate was estimated to be ~12 nm/min.

Optical properties

Figure 4 shows optical transmittance spectra of electrodeposited ZnO films without and with the pretreatment. For the ZnO film prepared by the sole galvanostatic deposition, the transmittance level was low in the visible range (~20–40%) and the absorption edge was not sharp. Such behavior was closely related to the lower density of ZnO film. For ZnO films prepared with the pretreatment, higher transmittance in the visible band (~60–90%) and sharp absorption edge located at about 370 nm were obtained, which was consistent with the behavior of a homogeneous semiconductor film. The highest optical transmittance (80–90%) was observed in the film with the pretreatment at

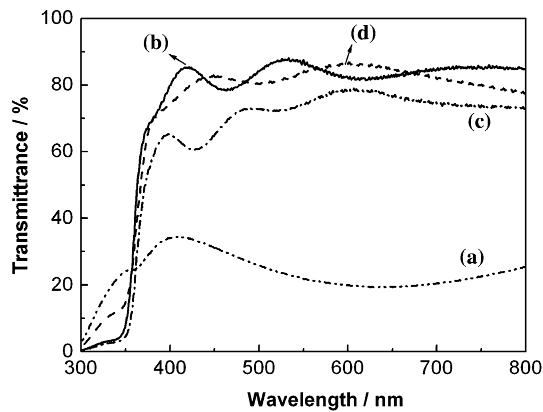

Fig. 4 Optical transmittance spectra of electrodeposited ZnO films prepared with different pretreatment conditions: (**a**) without pretreatment, (**b**) –1.2 V, 15 s, (**c**) –1.4 V, 15 s, (**d**) –1.2 V, 5 s. *Note*: Film thickness 250 nm for (**b**)–(**d**)

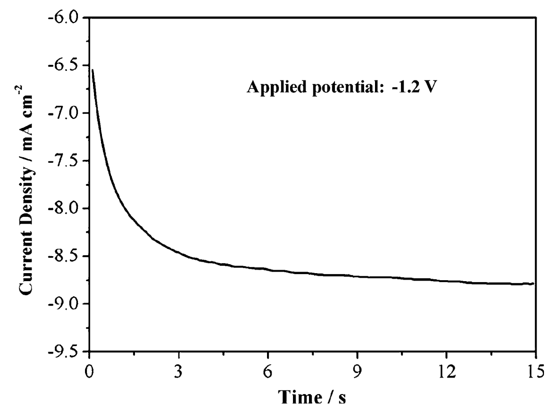

Fig. 5 Current-time curves recorded at the potential of –1.2 V for 15 s during the pretreatment process

–1.2 V for 15 s, which agrees well with its smaller grains and smooth surface in this film. It should be noticed that the transmittance of ITO substrate (200 nm) is 83% in the visible band. For more negative potential, there was a slight decrease in the transmittance due to the increase of the crystallite size. For shorter (5 s) or longer (60 s, not shown) pretreatment time, there was also a slight decrease in the transmittance. It may be due to the increased light scattering, which was brought by more irregular surface and the existence of some defects such as pores in obtained film as shown in Fig. 3.

Analysis on growth mechanism

Above experimental results suggested that, the potentiostatic pretreatment of the substrate plays a crucial role in the formation of dense ZnO layers. Then it is very interesting to investigate how this short process affects the growth process of ZnO films. Here by examining the current-time curve during the potentiostatic process and the potential-time curve during the galvanostatic process, together with the morphological change of ZnO films grown at the initial growth stage, we have made a preliminary exploration on the nucleation and growth process of ZnO on pretreated layer.

Figure 5 gives the current density-time curve during the pretreatment process at the potential of –1.2 V for 15 s. The current density increased progressively at the beginning and then tended to a stationary value. Mainly two processes occurred in this pretreatment: the charging of the electrode-precursor interface (causing the increase of conductivity), and the reduction of NO_3^- group (resulting in the ultimate formation of ZnO, and the decrease of conductivity). So the current density-time curve recorded in the pretreatment process was the integrative function of the two factors. Figure 7a and b illustrated SEM images of ITO substrates before and after the pretreatment. It can be seen clearly that the pretreatment process can produce high-density nuclei with the size of about 20 nm on the substrate, which agreed well with the study of Fujimura et al [27]. The ZnO seed layer produced in the pretreatment process will have significant effects on the growth of ZnO in the subsequent stage.

Figure 6 displays the potential-time curves of ZnO film without pretreatment (Fig. 6a) and with pretreatment at –1.2 V for 15 s (Fig. 6b) recorded in the galvanostatic deposition stage. For the case without the pretreatment, an abrupt inflexion during the first 100 s was observed, and after that, the potential decreased to a stationary value (~–0.8 V). For the case with the pretreatment, no initial inflexion was detected, and the potential increased progressively with the deposition time. This result indicates that the nucleation process occurred on the treated and untreated substrate is completely different. For the case

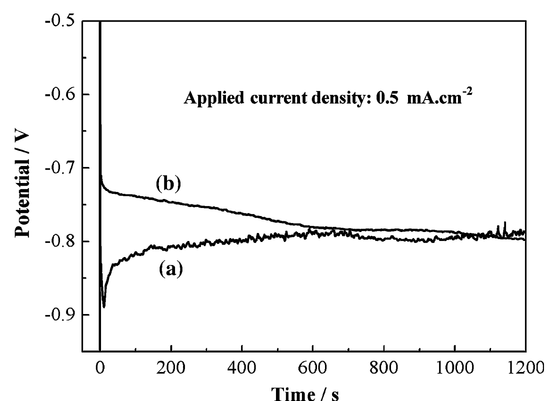

Fig. 6 Potential-time curves recorded (**a**) without pretreatment and (**b**) with pretreatment at –1.2 V for 15 s during the deposition at –0.5 mA for 20 min

Fig. 7 Growth process of the ZnO films observed by SEM: (a) bare ITO substrate, (b) after pretreatment at –1.2 V for 15 s, (b) after deposition at –0.5 mA for 5 min

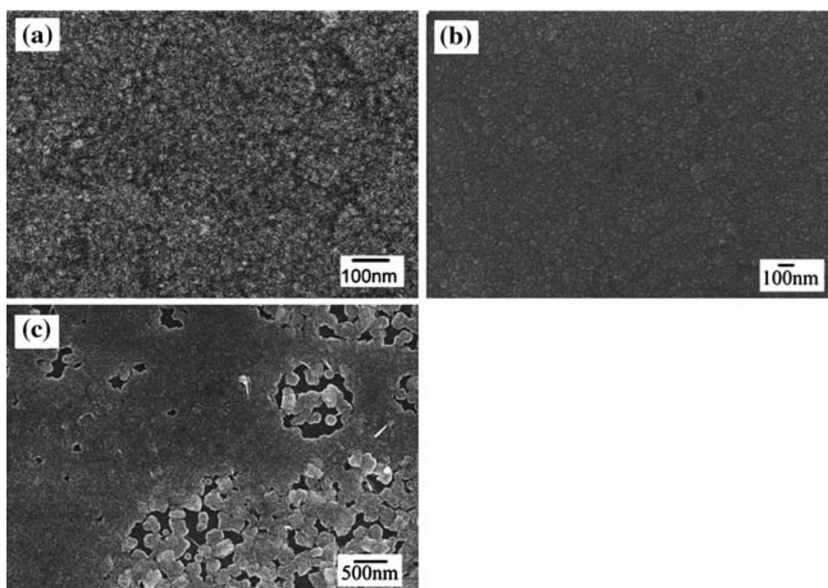

without the pretreatment, the nucleation took place on the substrate in the galvanostatic deposition stage, corresponding to the abrupt inflexion in curve (a). Since the applied voltage was relatively low compared with that in the pretreatment case, the nuclei density was low and the distribution of ZnO grains on substrate was sparse. So the conductive property changed hardly with the progress of ZnO growth, corresponding to the decreasing and steady V-t curve (Fig. 6a). In contrast, for the case with the pretreatment, the nucleation of ZnO has completed in the pretreatment process. So the nucleation on substrate was not necessary in the galvanostatic stage, and the growth of ZnO crystals took place directly on already-formed nuclei. The increase of the potential with the time indicates the conductivity decrease of the electrode-ZnO layer, which may be resulted from the coalescence of ZnO crystallites after the initial nucleation and growth stage [27, 28].

Figure 7c shows the surface morphology of ZnO films grown for 5 min on pretreated substrate (–1.2 V for 15 s). Both the continuous ZnO layer and jointed ZnO nanoparticles can be observed. This may support such following growth mode of ZnO film on pretreated ITO substrate: (1) Large ZnO particles were grown from minute ZnO crystallites on substrate produced by the electrochemical pretreatment; (2) Neighboring ZnO particles coalesced each other, forming the continuous ZnO layer; (3) Subsequent crystallites grew on already-formed continuous ZnO layer, increasing the film thickness to the desired value. In contrast, for the case without the pretreatment, the formation of loosely-dispersed ZnO rods may be resulted from the absence of ZnO seed layer and the growth of electrodeposited ZnO crystallites on already-formed ZnO crystallites instead of on substrate.

Conclusions

Compact and transparent ZnO film has been successfully deposited on ITO substrate by the galvanostatic deposition with the potentiostatic pretreatment process for a short time. The obtained films show high-preferred orientation along (002) plane, dense film structure and high optical transmittance higher than 80% in the visible band. The orientation of ZnO film was found to be closely related to the substrate etching in diluted HCl solution. The pretreatment conditions such as the potential and time have remarkable influence on the crystallinity and microstructure of ZnO films, and the optimal pretreatment condition is –1.2 V for 15 s. The analysis on the growth mechanism indicates that the potentiostatic pretreatment at more cathodic potential can substitute the initial nucleation process in the conventional one-step galvanostatic deposition, and significantly increase the nuclei density on substrate.

Acknowledgements This work is financially supported by National Natural Science Foundation of China (50502038), Shanghai Natural Science Foundation (05ZR14132), Shanghai-Applied Materials Research and Development Fund (06SA07), and State Key Laboratory of High Performance Ceramics and Superfine Microstructure (SKL200505SIC).

References

1. Peulon S, Lincot D (1996) Adv Mater 8:168
2. Gal D, Hodes G, Lincot D, Schock HW (2000) Thin Solid Films 361–362:79
3. Izaki M, Omi T (1996) Appl Phys Lett 68:2439
4. Stott L, Hedström J, Rückh M, Kessler J, Velthaus KO, Schock HW (1993) Appl Phys Lett 62:597

5. Ikeda T, Sato J, Hayashi Y, Wakayamma Y, Adachi K, Nishimura H (1994) Sol Energy Mater Sol Cells 24:379
6. Sen S, Leary DJ, Bauer CL (1982) Thin Solid Films 94:7
7. Chen Y, Bagnall DM, Zhu Z, Sekiuchi T, Park K, Hiraga K, Yao T, Koyama S, Shen MY, Goto T (1997) J Crystal Growth 181:165
8. Zhao JL, Li XM, Bian JM, Yu WD, Gao XG (2005) J Crystal Growth 276:507
9. Kasuga M, Takano T, Akiyama S, Hiroshima K, Yano K, Kishiom K (2005) J Crystal Growth 275:1545
10. David T, Goldsmith S, Boxman RL (2004) Thin Solid Films 447/448:61
11. Bian JM, Li XM, Gao XD, Yu WD, Chen LD (2004) Appl Phys Lett 84:541
12. Pauporté Th, Lincot D (2000) Electrochimica Acta 45:3345
13. Mahalingam T, John VS, Raja M, Su YK, Sebastian PJ (2005) Sol Energy Mater Sol Cells 88:227
14. Mei YF, Siu GG, Fu RKY, Chu PK, Li ZM, Tang ZK (2006) Appl Surf Sci 252:2973
15. Marotti RE, Giorgi P, Machado G, Dalchiele EA (2006) Sol Energy Mater Sol Cells 90:2356
16. Marotti RE, Guerra DN, Bello C, Machado G, Dalchiele EA (2004) Sol Energy Mater Sol Cells 82:85
17. Inamdar AI, Mujawar SH, Sadale SB, Sonavane AC, Shelar MB, Shinde PS, Patil PS (2007) Sol Energy Mater Sol Cells 91:864
18. Rairez D, Silva D, Gomez H, Riveros G, Marotti RE, Dalchiele EA, Sol Energy Mater Sol Cells (in press, doi:10.1016/j.solmat.2007.04.017)
19. Fahoume M, Maghfoul O, Aggour M, Hartiti B, Chraibi F, Ennaoui A (2006) Sol Energy Mater Sol Cells 90:1437
20. Peulon S, Lincot D (1998) J Electrochem Soc 145:864
21. Goux A, Pauporté T, Chivot J, Lincot D (2005) Electrochimica Acta 50:2239
22. Pauporté T, Lincot D (2001) J Electrochem Soc 148:C310
23. Weng J, Zhang YJ, Han GQ, Zhang Y, Xu L, Xu J, Huang XF, Chen KJ (2005) Thin Solid Films 478:25
24. Izaki M (1999) J Electrochem Soc 146:4517
25. Klug HP, Alexender LE (1974) X-ray diffraction procedures for polycrystalline and amorphous materials. Wiley, New York
26. Studenikin SA, Golego N, Cocivera M (1998) J Appl Phys 83:2104
27. Fujimura N, Nishihara T, Goto S, Ito T (1991) J Crystal Growth 55:816
28. Pauporté Th, Lincot D (2001) J Electroanalytical Chem 517:54